Virchows Arch [Pathol Anat] (1983) 400:173–186

Virchows Archiv A

A morphometric analysis of the hypertrophy of experimental liver cirrhosis

Jei W. Ryoo, and Robert J. Buschmann
Departments of Pathology, University of Illinois at the Medical Center and Veterans Administration West Side Medical Center, P.O. Box 8195, Chicago, Illinois 60680, USA

Summary. The objective of this study was to better elucidate the composition of the hypertrophic cirrhotic liver. We induced cirrhosis with hypertrophy in rats by simultaneous treatment with CCl_4 and phenobarbital (PB) and devised a hierarchy of structure applicable to the sampling and morphometric analysis of untreated and PB-treated control livers and of cirrhotic livers. Our analysis demonstrated that the hepatomegaly attributable to cirrhosis is virtually the total result of an increase in the specific volume (ml/100 g body weight) of the non-parenchyma, most of which is connective tissue and vascular lumen volume. Inconsequential to the hepatomegaly but statistically significant were the volumetric increases found in the following parenchymal compartments: hepatocyte nucleus, Kupffer/endothelial cell nucleus, Ito cell nucleus and cytoplasm, and bile canaliculus. The change in the hepatocyte nucleus is the result of an increase in size rather than in number. Sinusoidal space is the only compartment that showed a significant decrease. This study shows the practicality and usefulness of applying morphometric methods to cirrhotic liver.

Key words: Liver cirrhosis – experimental – Carbon tetrachloride – Hypertension – portal – Stereology – Hepatomegaly

Introduction

Although an atrophic cirrhotic liver must have less than the normal amount of parenchyma, it is not apparent what comprises a hypertrophic cirrhotic liver. Cirrhosis with hypertrophy is generally believed to indicate an early stage of the cirrhotic process and, presumably having more parenchyma, is assumed to have a better prognosis than a cirrhosis with atrophy (Sherlock

Offprint requests to: R.J. Buschmann at the above address

Supported in part by the Medical Research Service of the Veterans Administration

1981). Authors of chapters (McSween 1976; Edmondson and Peters 1977) in general pathology textbooks suggest that the response of the hepatocyte is responsible for the enlargement of the cirrhotic liver. A hypothetical cause and mechanism of hepatic regeneration and hypertrophy has been given (Zimmon 1977). Galambos (1979), on the other hand, doubts that an actual increase of normally functioning parenchyma is present in a hypertrophic liver with cirrhosis no matter how large the liver is.

A functional study (Pirttiaho et al. 1978) of biopsy specimens from hypertrophic livers of alcoholics with cirrhosis suggests that the liver enlargement compensates for a decreased cytochrome P450 concentration (nmol/gm of tissue), but no direct evidence for the implied increase of parenchyma is given. Another study (Bircher et al. 1973) which used a different measure of function suggests that the enlargement is due mainly to addition of non-functioning liver volume. The study, however, does not determine whether the non-functioning liver volume is comprised of new blood vessels, additional connective tissue, or functionally-compromised hepatocytes which are increased in number or size. A morphometric study (Nakamura et al. 1965) on human biopsy specimens shows more connective tissue in the large cirrhotic livers, but no assessment of the parenchymal contribution was made. Another morphometric study (Ludwig and Elveback 1972) on autopsy specimens reveals no increase of parenchymal tissue in the enlarged liver with cirrhosis which suggests that an increase of non-parenchymal tissue accounts for the enlargement.

The above-cited evidence demonstrates that considerable confusion and ambiguity about the composition of the hypertrophic cirrhotic human liver exists. These may be the result of extrapolating from indirect observations or observing etiologically and morphologically different types of human cirrhoses at various stages. These compromising factors can be largely overcome by using an animal model of liver cirrhosis. Although such a model may not mimic exactly all the features of human cirrhoses, the essential features, namely, nodular parenchyma and formation of septa (Popper 1977), are present. In our study we have determined the cellular, interstitial, and vascular and biliary luminal components that are responsible for the hypertrophy of the liver in one such model. In addition, we assessed the size and number of hepatocytes.

Materials and methods

Animal model, organ volumetry and tissue processing

Twenty-four male Holtzman rats each weighing 200–250 gm were divided into 3 equal groups and were housed 4 rats per cage. All animals were fed with commercial rat pellet chow and had free access to drinking water. One group was treated simultaneously with sodium phenobarbital (PB) and CCl_4 for 8 weeks following the protocol established by McLean et al. (1969) (CCl_4 + PB-treated group). We used a 45 l box for the gassing with CCl_4. Two rats, one from each cage of this group, died during the early period of the inhalation treatment. The second group was treated only with PB (PB-treated control group). The third group was an untreated control group. Four days after the final (16th) exposure to CCl_4, the treated

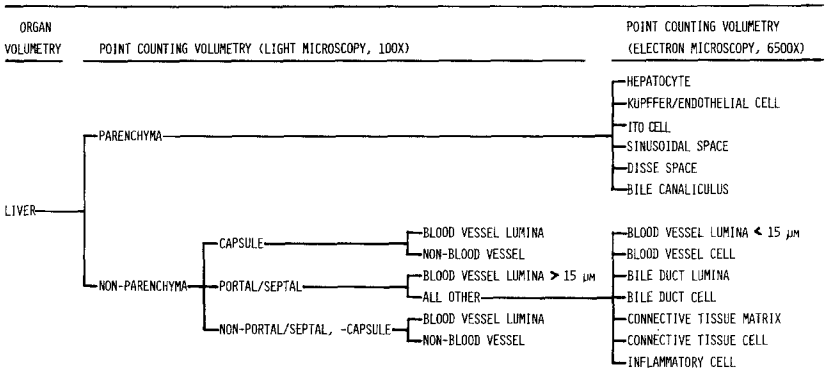

Fig. 1. Hierarchy of the liver compartments that were stereologically analyzed. Although not indicated in this figure, the nuclear and cytoplasmic compartments of each cell type were also analyzed

animals and their controls were anesthetized with Nembutal; the portal veins were cannulated; and the cannulas were held in place by a ligature around the cannulas, portal vein, and inseparable hepatic artery. After severing the vena cava, the livers were perfused at a hydrostatic pressure of 20 ± 3 mm Hg, at first, briefly (30 s) with heparinized saline (1,000 units/ml), and finally with 1.5% glutaraldehyde in 0.1 M phosphate buffer, pH 7.4, for 5 min (Blouin et al. 1977). A total of 5 well-perfused livers was obtained for each of the three groups.

Immediately following perfusion each liver was removed intact from the animal and weighed, and then the left lobe was separated and weighed. Although cirrhosis formation was unequal among the liver lobes, the left lobe represented a more or less average involvement. Moreover, a statistical analysis showed that the weight of the left lobe was well-correlated ($r = 0.97$) to the weight of the whole liver in both treated and untreated animals and that this lobe was also the best fixed. Therefore, we have assumed for this study that the left lobe is representative of the whole liver. A large wedge-shaped sample was taken from the left lobe, diced to 1 mm^3, and routinely processed and embedded in epoxy resin. The specific gravity of the liver was estimated from the weight and volume of the remaining left lobe (Scherle 1970). The volume of the whole liver was then calculated from its weight and the specific gravity. The remaining left lobe was subsequently processed and embedded in the Sorvall Embedding Medium (DuPont Co., Newtown, CT. USA) for light microscopy.

Morphometric compartments

A hierarchy of histological and ultrastructural compartments that were common to both normal and cirrhotic livers was devised (Fig. 1). While the definition and morphological criteria for most compartments are self-explanatory, the following remarks need to be noted. Our hierarchy of parenchymal components is essentially the same as that of Blouin et al. (1977) except that we did not differentiate the sinusoidal lining cells as either Kupffer cells or endothelial cells because, in our opinion, the difference is often equivocal particularly when encountering the smaller profiles of either cell. We assumed that any cell within the Disse space is an Ito cell. Interhepatocyte space except for the bile canaliculus was considered part of the Disse space. Fibrous tracts less than about 4.4 µm in thickness were empirically determined to be virtually unresolvable by light microscopy and, therefore, when encountered by electron microscopy they were considered part of the parenchyma, specifically part of the space of Disse. The non-portal/septal, non-capsule compartment contains the hepatic vein vessels except those that may have been incorporated into septa. No attempt was made to distinguish lymphatic capillaries from blood capillaries.

Stereology

The volume fraction of each compartment was determined by point counting stereological methods (Weibel 1979). The reference area for the compartments counted by light microscopy was the entire liver; the reference area for the compartments counted by electron microscopy was either a parenchymal, a portal, or a septal area. For point counting by light microscopy, we used an eyepiece reticle engraved with a square lattice test system (American Optical, Buffalo, NY, USA) which had a distance between lines equivalent to 100 μm on the 100× image of the histological section and which had a total of 121 points. We counted 20 adjacent, non-overlapping fields of view on one section from each of 5 blocks of embedded tissue from each animal. For ultrastructural analysis, 5 randomly selected blocks of tissue were thin-sectioned for each cirrhotic liver, 15–18 consecutive, non-overlapping electron micrographs were taken from a random area of one section of each block, and the compartments within parenchymal and septal areas point-counted. For each control liver, 3 randomly selected blocks of tissue were thin-sectioned, 15–19 consecutive, non-overlapping electron micrographs were taken from a random area of one section of each block, and the compartments within the parenchymal area were point-counted. In addition, 3 blocks of tissue were chosen for the presence of a portal area which was then thin-sectioned. A maximum number of non-overlapping electron micrographs of the portal area was taken from one section of each block (this provided 13–33 electron micrographs per animal), and the compartments within the portal areas were point-counted. For point counting we used a transparent sheet engraved with a square lattice test system which had a distance between lines equivalent to 3.46 μm on the 6,500× electron micrographs and which had a total of 99 points.

The volume fraction of each compartment was calculated for each animal by dividing the sum of all points that fell on the compartment by the sum of all points that fell on the containing reference area. The specific volume (absolute volume per liver per 100 gm body weight) of each compartment for each animal was calculated from the volume fraction, total liver volume, and animal body weight.

The numerical density (N_v) of hepatocyte nuclei was calculated from data obtained from an epoxy-embedded, toluidine blue-stained section of liver from each of the 5 blocks from each animal in each group. Sections were cut at a thickness, t, equal to 1 μm. By camera lucida all hepatocyte nuclear profiles and parenchymal area boundaries were drawn within a 15×15 cm areal test frame which represented 10,000 μm^2 at 1,500× (Fig. 2). Approximately 120 test areas were analyzed per animal from which an average of 1,100 nuclear profiles was counted. The overestimation due to edge effect was compensated for by the method of Gundersen (1977). The areas of 300–400 of these nuclear profiles which were randomly selected and the areas of parenchyma were measured with a computer-interfaced, x−y digitizing tablet that is a part of Bioquant II (R&M Biometrics, Nashville, TN, USA). Nuclear diameters were calculated from the nuclear areas which were assumed to be circles. From a distribution of these nuclear profile diameters for each animal, an average true diameter, D, was derived after correcting for lost profiles and section thickness according to the procedure given by Weibel (1979) in his section 5.2.4. The correction for lost profiles was subsequently applied to the number of nuclei counted in order to give a truer number of nuclei, N. The hepatocyte area, A, in which the nuclei were counted was calculated by multiplying the measured parenchymal area by the volume fraction of hepatocytes per parenchyma. The following formula (Abercrombie 1946; Weibel 1979) was used to calculate the nuclear numerical density per unit volume of hepatocyte for each animal:

$$N_V = \frac{N_A}{\bar{D} + t}.$$

The reciprocal of this numerical density is the average hepatocyte volume per nucleus. The specific number of hepatocyte nuclei was calculated by multiplying N_v by the specific hepatocyte volume.

Statistical analysis

The animal means among the three treatment groups were statistically compared by an analysis of variance. We compared the two control groups with the CCl_4 + PB-treated group and

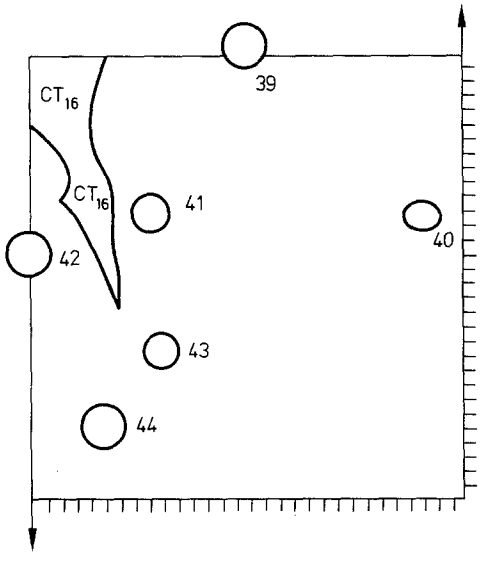

Fig. 2. Areal test frame and camera lucida drawing. Hepatocyte nuclear profiles are numbered and non-paranchymal areas are outlined (CT). The forbidden lines of Gundersen (1977) are the spiked edges and the arrowed lines extending from the square. Nuclear profiles touching any part of the forbidden lines were not counted or measured. Area of figure reduced to 0.15 of original

the untreated control group with the PB-treated control group by orthogonal comparison (Sokal and Rohlf 1981) in which a two-tailed F-test was used.

Results

Gross findings

The average body weights of the untreated control, PB-treated control, and CCl_4 + PB-treated animals were 442 ± 19.1, 511 ± 9.67 and 395 ± 19.5 gm ($\bar{X} \pm$ SEM), respectively. At laparatomy the livers of all the PB-treated control and CCl_4 + PB-treated animals were obviously hypertrophied; volumetry established their liver volumes as 22.7 ± 0.618 and 19.0 ± 0.618 ml ($\bar{X} \pm$ SEM), respectively, and that of the untreated control liver as 14.4 ± 1.21 ml. All CCl_4 + PB-treated animals had uniformly finely granular liver surfaces and had evidence of portal hypertension, namely splenomegaly, minor ascites and increased diameter of the portal vein and its intestinal afferents. Because of the increased diameter of the portal veins, catheterization was easier than in animals from the two control groups. Although we were apprehensive about encountering difficulty in perfusing cirrhotic livers, they proved to be consistently less resistant to the flow of perfusate than either of the control groups.

Histological and ultrastructural morphology

Sections of the livers from untreated control animals revealed a normal lobular architecture composed of one-cell-thick hepatic plates separated by open sinusoidal spaces. The portal veins were always patent and contained few, if any, blood cells unlike the accompanying hepatic arteries which

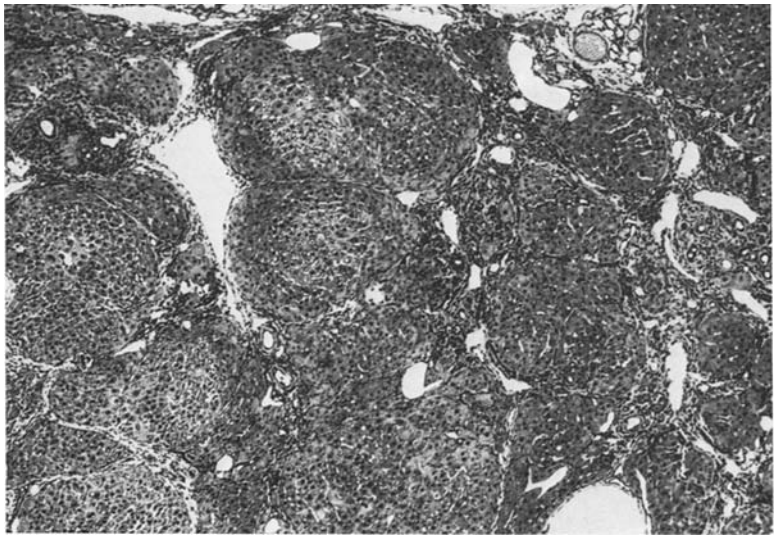

Fig. 3. Photomicrograph showing cirrhosis of the liver from CCl_4 + PB-treated animal. Hematoxylin and Eosin. (×46)

often were filled with blood cells. The livers from the PB-treated control animals showed light microscopic features virtually identical to the untreated control except that the hepatocytes, particularly around the central veins, were hypertrophic and contained cytoplasmic areas having a ground glass appearance. All sections from the livers of the CCl_4 + PB-treated animals demonstrated diffuse fibrous septa completely circumscribing nodules of hepatocytes (Fig. 3). Necrosis and significant fat were not evident. The septa had few inflammatory cells but contained numerous blood vessels of various sizes. The parenchymal nodules showed signs of regeneration, namely, disarrayed hepatic plates with thicknesses often greater than one cell and hepatocytes with binuclear profiles and mitotic figures. All of these features characterize cirrhosis as recently reiterated (Leevy et al. 1976; Popper 1977; Anthony et al. 1978). Most periseptal hepatocytes demonstrated a ground glass appearance of their cytoplasm much like that seen in the centrilobular hepatocytes of the PB-treated control.

The fine structure of the liver from the untreated control animals is well documented and need not be reiterated here. The most remarkable ultrastructural feature of the liver from animals treated chronically with phenobarbital either with or without CCl_4 was an increase in hepatocytic smooth endoplasmic reticulum. Additional remarkable features were present in the cirrhotic liver. The bile canaliculi had few microvilli, and the interhepatocytic microvilli and spaces were more abundant and wider, respectively, than those in the control livers. The interhepatocytic spaces were often seen to be continuous with the Disse space and, at time, also contained the cytoplasmic processes of Ito cells. In addition, the Ito cells appeared

most prominent in cirrhotic liver, and the Disse space contained noticeable amounts of collagen. The non-parenchyma of the cirrhotic liver, when compared to that of the two controls, appeared to have a proliferation of bile ducts, small blood vessels, and fibrous connective tissue. The fibroblasts had slender branches which were associated with collagen fiber bundles. Some of the fibroblasts contained a few fat droplets which were similar in size and density to those of Ito cells.

Morphometry

The mean specific volume (ml per 100 gm body weight) of the liver and each of its subcompartments is given for each of the 3 treatment groups in Table 1. The specific volume of the CCl_4 + PB-treated liver is significantly greater than that of the controls. In addition, the PB-treated control liver volume is significantly greater than the untreated control liver volume. Thus, both the cirrhotic and PB-treated control livers show true hepatomegaly although a comparison of the subcompartment volumes reveals different sources of the increased liver volume. In order to better and more easily appreciate the relationship of the volumes of the various subcompartments both within and among treatment groups, we have presented the data graphically (Fig. 4). In this figure the extent of the hepatomegaly of the PB-treated and CCl_4 + PB-treated animals is clearly represented by the greater overall length of their columns as compared to the column of the untreated control. In the case of PB-treated animals, the hepatomegaly was mainly due to the significant increase in the hepatocyte cytoplasmic compartment. In the case of CCl_4 + PB-treated animals, on the other hand, much of the hepatomegaly was due to significant volumetric increases in all portal/septal and capsular compartments of the non-parenchyma, especially in the portal/septal blood vessel lumina, connective tissue matrix, and connective tissue cells. Unlike the PB-treated control, additional increases were found in cirrhosis in the volume occupied by hepatocyte nuclei, Kupffer/endothelial cell nuclei, bile canaliculus, and Ito cell nuclei and cytoplasm. In addition, a significant decrease in the volume of sinusoidal space was detected in the cirrhotic liver.

Figure 5 graphically demonstrates the vascular volumes among the treatment groups. The cirrhotic livers had a significantly greater overall vascular volume than either that of the normal-sized liver from untreated control or that of the hypertrophic liver from the PB-treated control. The increased vascular volume in cirrhosis is evidently due primarily to the increased vasculature of the septum and minimally to the neovascularization of the capsule. There was a significant decrease in the volume of sinusoidal space.

Table 2 summarizes data for additional parameters of the hepatocytes for the three treatment groups. Cirrhotic livers give rise to a significant increase in nuclear diameter over both controls while PB-treatment alone gives rise to an increase in nuclear diameter over the untreated control. No change in the total number of hepatocyte nuclei per liver was demonstrated among the three treatment groups.

Table 1. Specific Volume as ml/100 g body weight ($\bar{X} \pm$SEM, $n=5$) for each liver compartment. An analysis of variance was used with an orthogonal comparison of the untreated plus PB-treated control groups with the CCl_4+PB treated group and of the untreated control group with the PB-treated control group

	Control (A)		PB Control (B)		CCl_4+PB (C)		$P<$*	
							(A) and (B) vs. (C)	(A) vs. (B)
Liver	3.25	(±0.160)	4.44	(±0.0515)	4.84	(±0.140)	0.002	0.002
Parenchyma	3.02	(±0.141)	4.16	(±0.0645)	3.60	(±0.125)		0.002
Hepatocyte	2.56	(±0.140)	3.63	(±0.0798)	3.09	(±0.0843)		0.002
Nucleus	0.146	(±0.00967)	0.168	(±0.00744)	0.219	(±0.0189)	0.01	
Cytoplasm	2.41	(±0.132)	3.46	(±0.0786)	2.87	(±0.0968)		0.002
Kupffer/Endothelial cell	0.0842	(±0.00875)	0.0822	(±0.00516)	0.104	(±0.0121)		
Nucleus	0.0152	(±0.00266)	0.0161	(±0.000702)	0.0257	(±0.00279)	0.01	
Cytoplasm	0.0690	(±0.00743)	0.0661	(±0.00502)	0.0783	(±0.0102)		
Ito cell	0.0210	(±0.00249)	0.0301	(±0.00331)	0.0809	(±0.00959)	0.002	
Nucleus	0.00522	(±0.00190)	0.00701	(±0.00143)	0.0159	(±0.00308)	0.01	
Cytoplasm	0.0158	(±0.00157)	0.0231	(±0.00229)	0.0651	(±0.00671)	0.02	
Sinusoidal space	0.266	(±0.0239)	0.292	(±0.0336)	0.183	(±0.0328)	0.05	
Disse space	0.0847	(±0.00731)	0.112	(±0.00970)	0.121	(±0.00770)		
Bile canaliculus	0.00511	(±0.00110)	0.0164	(±0.00429)	0.0229	(±0.00390)	0.05	
Non-parenchyma	0.234	(±0.0228)	0.273	(±0.0399)	1.24	(±0.122)	0.002	
Capsule	0.00887	(±0.00112)	0.00830	(±0.00207)	0.0686	(±0.00759)	0.002	
Blood vessel lumina	0		0		0.0115	(±0.00294)	–	–
Non-blood vessel	0.00887	(±0.00112)	0.00830	(±0.00207)	0.0571	(±0.00528)	0.002	
Portal/septal	0.123	(±0.0180)	0.149	(±0.0246)	1.07	(±0.0888)	0.002	
Blood vessel lumina >15 μm	0.0880	(±0.0141)	0.100	(±0.0198)	0.329	(±0.0265)	0.002	
Blood vessel lumina <15 μm	0.00214	(±0.000446)	0.00256	(±0.000669)	0.0601	(±0.00865)	0.002	
Blood vessel cells	0.00597	(±0.000785)	0.00857	(±0.00166)	0.0288	(±0.00391)	0.002	

Nucleus	0.00137	(±0.000174)	0.00182	(±0.000214)	0.00869	(±0.00140)	0.002
Cytoplasm	0.00460	(±0.000629)	0.00675	(±0.00148)	0.0203	(±0.00299)	0.002
Bile duct lumina	0.00173	(±0.000121)	0.00246	(±0.000489)	0.0127	(±0.00349)	0.002
Bile duct cells	0.00339	(±0.000315)	0.00505	(±0.000918)	0.0453	(±0.0114)	0.002
Nucleus	0.000992	(±0.000206)	0.00141	(±0.000304)	0.0124	(±0.00307)	0.002
Cytoplasm	0.00240	(±0.000248)	0.00364	(±0.000717)	0.0328	(±0.00836)	0.002
Connective tissue matrix	0.0273	(±0.0161)	0.0281	(±0.0105)	0.277	(±0.0391)	0.002
Connective tissue cells	0.0106	(±0.00220)	0.0135	(±0.000994)	0.303	(±0.0257)	0.002
Nucleus	0.00283	(±0.000627)	0.00421	(±0.000396)	0.0652	(±0.00727)	0.002
Cytoplasm	0.00778	(±0.00159)	0.00929	(±0.000617)	0.238	(±0.0205)	0.002
Inflammatory cells	0.000712	(±0.000103)	0.00103	(±0.000339)	0.0113	(±0.00317)	0.002
Nucleus	0.000215	(±0.0000368)	0.000141	(±0.0000658)	0.00422	(±0.00111)	0.002
Cytoplasm	0.000497	(±0.0000748)	0.000887	(±0.000314)	0.00710	(±0.00231)	0.01
Non-portal/Septal, -capsule	0.102	(±0.0277)	0.116	(±0.0235)	0.0998	(±0.0472)	
Blood vessel lumina	0.0863	(±0.0260)	0.0994	(±0.0223)	0.0809	(±0.0418)	
Non-blood vessel	0.0155	(±0.00260)	0.0161	(±0.00151)	0.0189	(±0.00627)	

* Unlisted p values are greater than 0.05 based on a two-tailed F-test

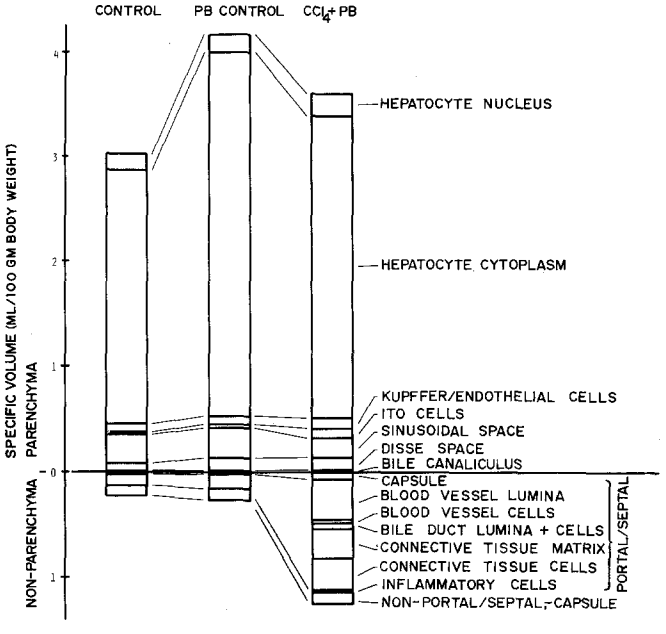

Fig. 4. Graphic presentation and comparison of the specific volumes of the various analogous compartments in the three treatment groups

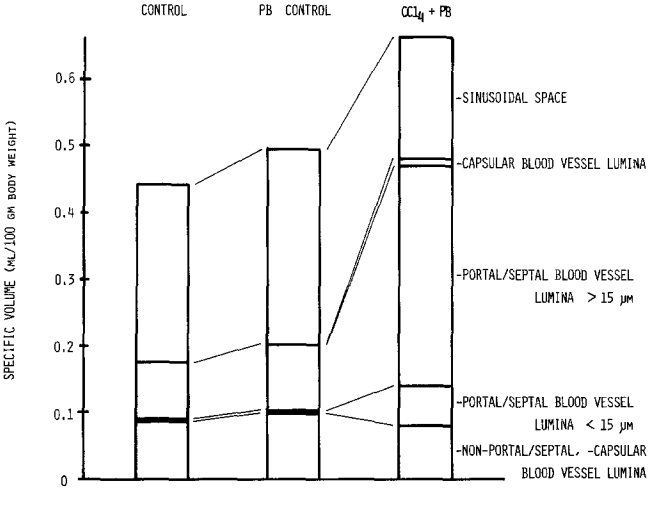

Fig. 5. Graphic presentation and comparison of the specific volumes of the vascular components of the three treatment groups

Discussion

Our simultaneous administration of CCl_4 and PB for 8 weeks according to McLean et al. (1969) produced in every animal hepatomegaly with an unequivocal cirrhosis (Fig. 3). The adequacy of our sample sizes, which are listed in the Materials and Methods section, is attested to by the many parameters that show significant differences. These differences demonstrate the major morphometric changes in the cirrhotic liver which is the purpose

Table 2. Parameters of hepatocytes ($\bar{X} \pm$SEM, $n=5$). An analysis of variance was used with an orthogonal comparison of the untreated plus PB-treated control groups with the CCl_4 + PB-treated group and of the untreated control group with the PB-treated control group

	Control (A)	PB-Control (B)	CCl_4 + PB (C)	$P<$*	
				(A) and (B) vs. (C)	(A) vs. (B)
Nuclear diameter, $\bar{D}$ (μm)	7.83 ± 0.53	8.72 ± 0.113	9.20 ± 0.072	0.002	0.002
Hepatocyte volume per nucleus (μm^3)	5,850 ± 249	9,240 ± 235	7,040 ± 681		0.002
Specific number of hepatocyte nuclei ($\times 10^6$ per 100 g body weight)	437 ± 13.1	394 ± 12.4	451 ± 33.8		

* Unlisted p values are greater than 0.05 based on a two-tailed F-test

of our study. Although additional sampling at any of the various levels (points, fields, blocks) which comprise the primary data for each animal will improve the chances of establishing further differences, as will increasing the number of animals per treatment group, these differences would not be important for establishing the major components of hypertrophy in cirrhosis.

Although significant morphometric changes are found in the parenchyma, the hepatomegaly attributable to cirrhosis is virtually the total result of an increase in the specific volume of the non-parenchyma which is essentially the morphometric representation of the septa of the cirrhotic livers. The major elements of this increase are both large (>15 μm) and small (<15 μm) blood vessels, connective tissue matrix, and connective tissue cells. The finding of fat droplets in many of the connective tissue cells of the septa is consistent with the idea that at least some of these cells may arise from Ito cells (Kent et al. 1976; Jacques et al. 1979). Some of the increased quantity of large blood vessels probably represents the shunt pathway demonstrated by Wood et al. (1979) to exist in the CCl_4 + PB-induced cirrhotic liver.

Although the total parenchymal contribution to the hepatomegaly of cirrhosis is not significant, remarkable morphometric changes, nevertheless, are seen. There is a volumetric increase in hepatocyte cytoplasm in the cirrhotic liver, but this effect cannot be disassociated from phenobarbital treatment. The ground glass hepatocytes that we observed in the periseptal zone of the nodules of the cirrhotic liver and that we and others (Burger and Herdson 1966; Massey and Butler 1979; Romagna and Zbinden 1981) observed in the centrilobular zone of livers from PB-treated animals would seem to be the major source of the increases in the respective hepatocyte cytoplasmic volumes. These observations further support a homology between the hepatocytes of Rappaport's zone 3 (Rappaport 1976) in normal

liver and the periseptal hepatocytes in cirrhotic liver (Nuber et al. 1980). The significant increase in hepatocyte nuclear volume is the result of an increase in size rather than number (Table 2). This enlargement may be related to polyploidy (Morselt et al. 1976). It would thus appear that, at least at this stage of cirrhosis, the hepatocytes that had evidently been lost as a result of CCl_4 toxicity have been restored essentially cell for cell.

The most striking finding in the parenchyma of the cirrhotic liver is the 3–4 fold increase in the specific volume of both the nuclear and cytoplasmic components of the Ito cells. Their increases and their association with the presence of abundant collagen fibers are further circumstantial evidence for the concept that the Ito cell is responsible for intralobular fibrosis (McGee and Patrick 1972; Kent et al. 1976). The volume of the bile canaliculi in the cirrhotic liver is significantly increased, and morphological examination shows loss of microvilli in this tissue. Therefore, the increase seems to be better attributed to swelling rather than to increased number of bile canaliculus profiles.

Our interest in vascular volume stems from our observation that a faster flow of perfusate occurred in cirrhotic livers than in any of the control livers. We had expected, in fact, a slow flow of perfusate and possibly even incomplete fixation of the cirrhotic liver. Our expectation was based on the presumption that an increased resistance caused the portal hypertension that we observed in all of our animals with cirrhosis. The inference from our results, on the contrary, is that less vascular resistance is present, and this may be related to the morphometrically determined increase in vascular volume in the cirrhotic liver (Fig. 5). The portal hypertension would then have to be attributed to other factors such as 1) increased afferent blood flow into the portal vein and 2) high hepatic arterial blood pressure conducted into the portal vein through cirrhosis-induced arteriovenous anastomoses (Koo et al. 1976) to which we have already attributed the significant increase in septal blood vessel lumina >15 μm (Table 1 and Fig. 5). Any portal hypertension due to either of the above two factors would have been eliminated by our ligation of the portal vein and hepatic artery during perfusion catheterization, thus accounting for the more rapid perfusate flow in the cirrhotic livers.

The salient features of hypertrophic liver cirrhosis that we derive from this morphometric study are the maintenance of normal hepatocyte number and a hepatomegaly essentially due to an increase in non-parenchymal volume, most of which is connective tissue and vascular lumen volume. Our conclusions are not at variance with the few morphometric data from human liver cirrhosis (Nakamura et al. 1965; Ludwig and Elveback 1972), but the extrapolation of our conclusions needs to be tested by a morphometric study similar to ours applied to autopsy material or possibly with limitations to available surgical wedge biopsy specimens. Our study, furthermore, does not permit insight into subcellular differences between cirrhotic and control liver which may be able to explain demonstrated functional differences. Our study does, however, provide a workable methodology and the necessary underlying data to carry out such studies.

Acknowledgements. The authors wish to thank Dean Manke, Judith Prostka, Ruth Hostler and Joyce Geoffroy for their technical assistance and Farris Brookshire for his typing of the manuscript.

References

Abercrombie M (1946) Estimation of nuclear population from microtome sections. Anat Rec 94:239–247

Anthony PP, Ishak KG, Nayak NC, Poulsen HE, Scheuer PJ, Sobin LH (1978) The morphology of cirrhosis. Recommendations on definition, nomenclature, and classification by a working group sponsored by the World Health Organization. J Clin Pathol 31:395–414

Bircher J, Blankart R, Halpern A, Häcki W, Laissue J, Preisig R (1973) Criteria for assessment of functional impairment in patients with cirrhosis of the liver. Eur J Clin Invest 3:72–85

Blouin A, Bolender RP, Weibel ER (1977) Distribution of organelles and membranes between hepatocytes and nonhepatocytes in the rat liver parenchyma. A stereological study. J Cell Biol 72:441–455

Burger PC, Herdson PB (1966) Phenobarbital-induced fine structural changes in rat liver. Am J Pathol 48:793–807

Edmondson HA, Peters RL (1977) Liver. In: Anderson WAD, Kissane JM (eds) Pathology. 7th ed, CV Mosby, St. Louis, pp 1321–1438

Galambos JT (1979) Cirrhosis. WB Saunders, Philadelphia, p 52

Gundersen HJG (1977) Notes on the estimation of the numerical density of arbitrary profiles: the edge effect. J Microsc 111:219–223

Jacques EA, Buschmann RJ, Layden TJ (1979) The histopathologic progression of vitamin A-induced hepatic injury. Gastroenterology 76:599–602

Kent G, Gay S, Inouye T, Bahu R, Minick OT, Popper H (1976) Vitamin A-containing lipocytes and formation of type III collagen in liver injury. Proc Natl Acad Sci USA 73:3719–3722

Koo A, Liang IYS, Cheng KK (1976) Effect of the ligation of hepatic artery on the microcirculation in the cirrhotic liver in the rat. Aust J Exp Biol Med Sci 54:287–295

Leevy CM, Popper H, Sherlock S (Criteria committee) (1976) Diseases of the liver and biliary tract: standardization of nomenclature, diagnostic criteria and diagnostic methodology. Fogarty International Center Proceedings, No 22 DHEW Publication No (NIH) 76-725. Government Printing Office, Washington, DC, pp 17–24

Ludwig J, Elveback LR (1972) Parenchyma weight changes in hepatic cirrhosis: a morphometric study and discussion of the method. Lab Invest 26:338–343

Massey ED, Butler WH (1979) Zonal changes in the rat liver after chronic administration of phenobarbitone: an ultrastructural, morphometric and biochemical correlation. Chem Biol Interact 24:329–344

McGee JO, Patrick RS (1972) The role of perisinusoidal cells in hepatic fibrogenesis: an electron microscopic study of acute carbon tetrachloride liver injury. Lab Invest 26:429–440

McLean EK, McLean AEM, Sutton PM (1969) Instant cirrhosis: an improved method for producing cirrhosis of the liver in rats by simultaneous administration of carbon tetrachloride and phenobarbitone. Br J Exp Path 50:502–506

McSween RNM (1976) Liver, biliary tract and exocrine pancreas. In: Anderson JR (ed) Muir's Textbook of Pathology. 10th ed Year Book, Chicago, pp 601–659

Morselt AFW, Freni SC, Ortlep FM (1976) Quantitative histological aspects of liver cirrhosis. Beitr Pathol 159:195–206

Nakamura T, Nakamura S, Aikawa T, Tazawa T, Suzuki O, Suzuki T (1965) Morphological classification of liver cirrhosis based upon measurement of per cent of interstitial tissue in liver biopsy specimens. Tohoku J Exp Med 87:110–122

Nuber R, Teutsch HF, Sasse D (1980) Metabolic zonation in thioacetamide-induced liver cirrhosis. Histochemistry 69:277–288

Pirttiaho HI, Sotaniemi EA, Ahlqvist J, Pitkänen U, Pelkonen RO (1978) Liver size and indices of drug metabolism in alcoholics. Eur J Clin Pharmacol 13:61–67

Popper H (1977) Pathologic aspects of cirrhosis: a review. Am J Pathol 87:228–264

Rappaport AM (1976) The microcirculatory acinar concept of normal and pathological hepatic structure. Beitr Pathol 157:215–243

Romagna F, Zbinden G (1981) Distribution of nuclear size and DNA content in serial liver biopsies of rats treated with N-nitrosomorpholine, phenobarbital and butylated hydroxytoluene. Exp Cell Biol 49:294–305

Scherle W (1970) A simple method for volumetry of organs in quantitative stereology. Microskopie 26:57–60

Sherlock S (1981) Diseases of the liver and biliary system. 6th ed, Blackwell, Oxford, p 331

Sokal RR, Rohlf FJ (1981) Biometry: The Principles and Practice of Statistics in Biological Research. 2nd ed. WH Freeman, San Francisco, pp 232–242

Weibel ER (1979) Stereological Methods, vol 1, Practical Methods for Biological Morphometry. Academic Press, London New York Toronto Sydney San Francisco

Wood AJJ, Villeneuve JP, Branch RA, Rogers LW, Shand DG (1979) Intact hepatocyte theory of impaired drug metabolism in experimental cirrhosis in the rat. Gastroenterology 76:1358–1362

Zimmon DS (1977) The hepatic vasculature and its response to hepatic injury: a working hypothesis. Yale J Biol Med 50:497–506

Accepted February 11, 1983